Chemical Geology 525 (2019) 28–36

Contents lists available at ScienceDirect

Chemical Geology

journal homepage: www.elsevier.com/locate/chemgeo

Adsorption of biologically critical trace elements to the marine cyanobacterium *Synechococcus* sp. PCC 7002: Implications for marine trace metal cycling

Brendan A. Bishop[a,*], Shannon L. Flynn[b], Tyler J. Warchola[a], Md. Samrat Alam[a,c], Leslie J. Robbins[a,1], Yuxia Liu[d], George W. Owttrim[e], Daniel S. Alessi[a], Kurt O. Konhauser[a]

[a] Department of Earth & Atmospheric Sciences, University of Alberta, Edmonton, Alberta T6G 2E3, Canada
[b] School of Natural and Environmental Sciences, Newcastle University, Newcastle upon Tyne NE1 7RU, United Kingdom
[c] Department of Physical and Environmental Sciences, University of Toronto at Scarborough, Toronto, Ontario M1C 1A4, Canada
[d] State Key Laboratory of Heavy Oil Processing, Beijing Key Laboratory of Oil and Gas Pollution Control, China University of Petroleum, Beijing 102249, China
[e] Department of Biological Sciences, University of Alberta, Edmonton, Alberta T6G 2E9, Canada

ARTICLE INFO

Editor: K Johannesson

Keywords:
Surface complexation modelling
Adsorption
Trace metal cycling
Cyanobacteria
Banded iron formation

ABSTRACT

Marine bacterial plankton play a key role in elemental cycling through their ability to bind, assimilate, metabolize, and modify the redox state of trace metals in seawater. Of those processes, arguably the least studied are the mechanisms underpinning trace metal adsorption to planktonic marine bacteria, despite a plethora of literature pertaining to terrestrial species. Recently, Liu et al. (2015) demonstrated that the marine cyanobacterium *Synechococcus* sp. PCC 7002 has the capacity to remove appreciable amounts of Cd^{2+}, a proxy for other divalent cations, from seawater by adsorption. In this study, we build on that work and employ a surface complexation modelling (SCM) approach using titration and pH adsorption edge experiments to calculate the thermodynamic binding constants of four bioessential transition metals (Co, Ni, Cu, Zn) to *Synechococcus* in simulated seawater. Based on the titration results, the major functional groups involved in metal binding were carboxyl groups with a pK_a of 5.59 and phosphoryl groups with a pK_a of 7.61. Metal adsorption experiments indicate that *Synechococcus* can bind considerable concentrations of Zn, Cu, Ni, and Co at pH 8. When all four metals are simultaneously added to solution, the same adsorption pattern of Zn > Cu > Ni > Co is maintained, and accurately predicted by the SCM. Based on average marine cell densities and turnover rates of *Synechococcus* cells in the photic zone, we calculate that *Synechococcus*, in the absence of competing ligands such as dissolved organic matter (DOM), has the theoretical capacity to remove nearly all of the free metal cations from seawater. These observations highlight the surface reactivity of marine cyanobacteria as a potentially important vector for the transfer of dissolved metals from the photic zone to deeper waters or the seafloor in modernoceans, but they also have implications for the Precambrian oceans as sinking cyanobacteria could have acted as an exit channel for trace elements into ancient sediments including banded iron formations (BIF).

1. Introduction

It has been demonstrated that planktonic cyanobacteria play an important role in primary production in the oceans, in particular, the genera *Synechococcus*, which has been estimated to contribute 17% of net marine primary productivity (Flombaum et al., 2013), with populations in the marine photic zone varying from 10^4 to 10^5 cells mL^{-1} (Waterbury et al., 1979; Worden et al., 2004; Huisman et al. 2018). Similar to other phytoplankton, these cyanobacteria play an important role in the cycling of trace metals (e.g., Mn, Fe, Co, Ni, Cu, Zn, and Cd) through: (1) the generation of reactive organic ligands on their cell walls which adsorb ions from seawater (Dittrich and Sibler, 2005), (2) assimilation for enzymatic use (Bruland et al., 1991; Morel and Price, 2003), (3) the production of extracellular ligands that complex trace metals and alter their bioavailability (Moffett and Brand, 1996; Worms et al., 2006; Fein, 2017), and (4) their production of dissolved organic matter upon cell lysis (Anderson and Tang, 2010; Carlson and Hansell, 2014). The net effect of these cellularly controlled processes is the

* Corresponding author at: Department of Earth & Atmospheric Sciences, University of Alberta, 1-26 University of Alberta, Edmonton, AB, Canada.
E-mail address: babishop@ualberta.ca (B.A. Bishop).
[1] Current address: Department of Geology and Geophysics, Yale University, New Haven, Connecticut, USA 06511.

https://doi.org/10.1016/j.chemgeo.2019.05.021
Received 6 September 2018; Received in revised form 8 May 2019; Accepted 15 May 2019
Available online 18 May 2019
0009-2541/ © 2019 Elsevier B.V. All rights reserved.

development of "nutrient-like profiles" where uptake by cyanobacteria depletes nutrients in the photic zone, with the nutrients returning to solution in deeper waters due to the degradation of bacterial biomass, and the eventual replenishing of the photic zone via upwelling currents (Morel, 2008; Sunda, 2012).

Twining and Baines (2013) proposed that the assimilation of trace metals reflect both their environmental availability as well as the biochemical demands of phytoplankton. The cellular assimilation of metals occurs by a two-step process in which metals first bind to surface ligands through adsorption, followed by their active transfer across the cell membrane (Morel et al., 1991; Fein, 2017). The assimilation of trace metals from seawater is critical for the cell as it requires metals for various metalloenzymes which are utilized in processes such as photosynthesis, nitrogen fixation, respiration, the uptake of other trace metals, and for accessing organic macronutrients (Morel et al., 1991; Twining and Baines, 2013). In some cases, metals can substitute for one another depending on their environmental availability; for example, *Thalassiosira weissflogii*, a marine diatom, can substitute Co and Cd for Zn (Price and Morel, 1990). In other cases entirely different proteins can be utilized if a required metal is falls below a biolimiting concentration (Twining and Baines, 2013).

Sañudo-Wilhelmy et al. (2004) found that phytoplankton are capable of adsorbing anionic trace nutrients such as phosphate, as well as cationic nutrients (e.g., Fe, Mn, and Mo) in laboratory settings using both simulated seawater and natural waters collected from the western Atlantic Ocean. The authors proposed that adsorption of cations to phytoplankton could be equally as important as uptake and assimilation by biological processes in controlling marine nutrient profiles. The ability of bacterial cell wall functional groups to react with protons and metal cations is well-established in the literature (e.g. Fein et al., 1997; Cox et al., 1999; Lalonde et al., 2008a; Alessi et al., 2010; Flynn et al., 2014). Although much of the current research has been directed at terrestrial microbes in order to better understand their potential for bioremediation, few studies have focused on planktonic marine cyanobacteria to determine their interactions with ions in seawater. In this regard, Dittrich and Sibler (2005) and Hadjoudja et al. (2010) demonstrated that marine cyanobacterial cell walls have low isoelectric points, as reflected by highly negative surface charges and low hydrophobicity, and therefore, are capable of efficiently adsorbing trace metals. Cyanobacteria, specifically those of the *Synechococcus* genera, have also been found to be capable of adsorbing trace metals due to their high surface area to volume ratio and highly reactive cell walls (Azam et al., 1983; Fisher, 1985).

More recently, Liu et al. (2015), Martinez et al. (2016), and Gélabert et al. (2018) investigated the surface reactivity of a marine cyanobacterium, an anoxygenic photosynthetic bacteria that oxidizes dissolved iron (a photoferrotroph), and marine and freshwater diatoms, respectively, and demonstrated that they are each capable of removing metal cations from seawater. The Liu et al. (2015) study aimed to provide a proof-of-principle, and therefore, only focused on a single metal cation and did not consider the competition among charged species for adsorption that would be expected in more complex environmental systems. Consequently, consideration of the effects of competitive adsorption is still needed to accurately represent the adsorption behaviour of trace metals in seawater. Accordingly, in this study, we extended the earlier work of Liu et al. (2015) by exploring the adsorption of a set of biologically important trace metals (e.g., Co, Ni, Cu, and Zn) onto *Synechococcus* sp. PCC 7002 using pH adsorption edge experiments. The resulting data were then used to develop surface complexation models (SCM) of single and multi-element adsorption systems. Metal binding constants derived from the SCM approach provide considerable advantages over more commonly employed empirical models of adsorption, as they can account for changing pH, ionic strength, and the presence of other sorbents and competing sorbates (Bethke and Brady, 2000; Koretsky, 2000). Developing such a modelling approach is critical in assessing the role of microbes as an exit channel for metals from seawater to marine sediments (Konhauser et al., 2018), and promises to yield more accurate and predictive models of metal speciation and modes of sequestration and cycling in modern and paleomarine settings.

2. Methods

2.1. Bacterial growth

The cyanobacterial strain *Synechococcus* sp. PCC 7002 (referred to hereafter as *Synechococcus*) was aerobically cultured on A+ medium (Stevens and Van Baalen, 1973; Stevens and Porter, 1980) (SI Table 1) agar plates with a light intensity of 50 mmol photons $m^{-2} s^{-1}$ at 30 °C for 14 days. Once a suitable colony developed on the plate, cells were harvested using an inoculation loop and inoculated in 50 mL of A+ media at 30 °C for 3 days. Cells were then transferred to a 1 L borosilicate Erlenmeyer flask with an additional 350 mL of A+ media and rotated at 100 rpm for 10 days until the stationary growth phase was reached. The stationary phase was selected for the experiments as the cells would be in equilibrium with the media, and the proton state surrounding the cell wall would be near equilibrium. Aeration was provided throughout by bubbling with filtered, humidified air. The cells were harvested by centrifugation at 10,000*g* for 8 min and washed with 0.56 M NaCl (a representative seawater concentration) five times to remove any residual growth media and competing metals from cell wall surface sites. Following each wash, the bacteria were resuspended in a fresh electrolyte solution and a new pellet of bacteria was formed by centrifugation and the supernatant was decanted. After the final wash, the bacteria were centrifuged twice for 30 min to remove as much water from the biomass as possible. The wet mass of bacteria was then determined gravimetrically, and the pelleted cells were suspended in 0.56 M NaCl.

2.2. Potentiometric titrations

Potentiometric titrations were conducted for comparison with the Liu et al. (2015) study in accordance with previously established protocols in our laboratory (e.g., Petrash et al., 2011; Warchola et al., 2017; Alam et al., 2018; Konhauser et al., 2019), in which the addition of aliquots of base induce the progressive deprotonation of organic functional groups at the bacterial surface. All plastic and glassware used for the titrations were soaked in 10% HCl for a minimum of 24 h, rinsed three times in 18.2 MΩ·cm water, and allowed to air-dry while inverted. Before each titration, 0.05 g (wet mass) of washed *Synechococcus* cells were suspended in 50 mL of 0.56 M NaCl, to achieve a final concentration of 2.5 g L^{-1}. Based on cell counts on a haemocytometer, 2.5 g L^{-1} is equivalent to 6×10^9 cells mL^{-1}. The titrations were conducted under a N_2 atmosphere and titration solutions were purged with N_2 gas for 30 min prior to commencement of the titration to establish and maintain a CO_2 free environment in the titration vessel. Throughout the titration, the pH was continuously measured using a glass electrode (Metrohm), calibrated in advance using commercially available buffers (Thermo Fisher Scientific). Titrations were performed alkalimetrically from pH 3 to 10 by initially acidifying the solution to pH 3 with 0.1 M HCl, followed by incremental additions of 0.1 M NaOH until pH 10 was reached. Previous studies have demonstrated that cell damage or lysis only becomes a factor at pH < 2 or pH > 10 (Borrok et al. 2005; Fein 2006), and therefore, is unlikely to affect the proton reactivity of *Synechococcus* cell surface functional groups. The volume of base added, and the corresponding pH change, were recorded for each titration step. A "down-titration" was then performed with the addition of 0.1 M HCl to pH 3 to determine the reversibility of proton binding and if hysteresis between the "up" and "down" titrations had occurred, which would be an indicator for titration-induced cell damage (SI Fig. 1). All titrations were performed in dynamic addition mode whereby the titrator adds a variable amount of either HCl or

NaOH depending on the instantaneous buffering capacity, as per Alam et al. (2018). Subsequent additions of acid or base were only made once the pH electrode achieved a stability of 0.2 mV s^{-1}. Blank titrations of the 0.56 M NaCl background solution were conducted to quantify the background proton buffering capacity, which was then subtracted from the *Synechococcus* titration data before modelling to determine cell wall functional group concentrations and proton binding constants (pK_a values).

The titration data was evaluated in terms of excess charge, where the reactivity of the background electrolyte was subtracted from the total reactivity of the solution so only the reactivity of the *Synechococcus* was modelled (Lalonde et al., 2008b; Lalonde et al., 2010). A least-squares optimization method was then applied using FITEQL v. 4.0 (Herbelin and Westall, 1999) to determine surface site acidity constants and ligand site concentrations based on the titration data.

2.3. Adsorption experiments

Adsorption experiments were conducted by measuring the change in the aqueous trace metal concentrations before, and after, exposure to pre-washed *Synechococcus* cells. The metal stock solutions were prepared by diluting a 1000 ppm standard solution of either Co, Ni, Cu, or Zn in 0.56 M NaCl to achieve a concentration of 10 ppm. A known mass of *Synechococcus* cells were suspended in the metal solution to achieve a wet mass concentration of 5 g L^{-1}. Aliquots of 10 mL of the bacteria-metal solution were then partitioned into 50 mL acid washed polypropylene test tubes and the pH of each was adjusted twice using aliquots of 0.01 M HCl or NaOH to bring the samples within the desired pH range of 3 to 9, at approximately 0.5 pH unit intervals. Each sample was mixed via end-over-end rotation at 40 rpm for 6 h to allow for equilibration between the metal-containing solution and the cellular surfaces.

Following equilibration, the final pH of each experiment was measured, and the solutions were centrifuged at 10,000*g* for 5 min to remove the cells. The supernatant was filtered through 0.2 µm nylon membranes and diluted 1:10 in 2% nitric acid before trace metal analysis by Inductively Coupled Plasma Mass Spectrometry (ICP-MS/MS) using an Agilent 8800. Before each analysis, a series of external standards prepared from commercially available ICP-MS standards were run. Controls containing the metal and 0.56 M NaCl background solutions were also analyzed to determine whether metal was lost by adsorption to the experimental apparatus.

Multi-element pH edges were performed using the same protocol as described above. However, to maintain a similar total metal concentration, 2.5 ppm of each of the four tested metals (Co, Cu, Ni, and Zn) were added, for a combined trace metal concentration of 10 ppm.

3. Results/discussion

3.1. Synechococcus surface reactivity

Fig. 1 shows the titration data for 2.5 g L^{-1} (wet mass) *Synechococcus* in 0.56 M NaCl electrolyte, plotted in terms of mmol of deprotonated sites (excess charge) per gram of bacteria. The slope at any point of the titration curve gives the instantaneous buffering capacity of the *Synechococcus* suspension at that specific pH, which corresponds to the rate of deprotonation of the surface ligands.

The titration data indicate that *Synechococcus* has a high buffering capacity over the pH range measured, with greatest changes in excess charge occurring at low (< 4.5) and high (> 8) pH values. Bacterial ligand concentrations and acid neutralizing capacity were determined from titration data using a pK_a spectrum approach similar to Lalonde et al. (2008a). The number of potential pK_a values is fixed in FITEQL 4.0 (Herbelin and Westall, 1999), which then optimizes for both the pK_a values and their corresponding site concentrations. The regions of the titration curve with the greatest slope represent regions in which the buffering capacity of the cells is greatest, and therefore, correlate with the functional group pK_a values. Minimal hysteresis was observed between the up and down titrations, indicating there was negligible cell damage and that the protonation and deprotonation of cell wall functional groups was highly reversible.

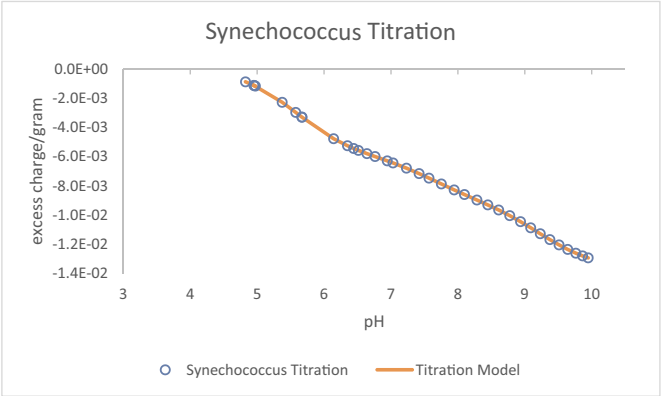

Fig. 1. Titration data in terms of excess charge per gram of Synechococcus cells, along with the FITEQL model best fit.

Protonation models with 1–4 sites were tested, and a model employing three proton active sites provided the best fit to the titration data. This result, combined with previous Fourier transform infrared (FTIR) spectroscopy performed on bacteria (Jiang et al., 2004; Yee et al., 2004; Liu et al., 2015), suggests that the bacterial cell surfaces have four primary types of proton-active functional groups, carboxyl groups which deprotonate at acidic pH values, phosphoryl groups which deprotonate at circumneutral pH, and amino and hydroxyl groups, both of which deprotonate at alkaline pH values.

The mass action equations for the deprotonation of each type of surface ligand can be described by the following balanced chemical reactions:

$$\equiv R - COOH + OH^- = R \equiv COO^- + H_2O \quad (1)$$

$$\equiv R - PO_4H_2 + OH^- = R \equiv PO_4H^- + H_2O \quad (2)$$

$$\equiv R - NH_3^+ + OH^- = R \equiv NH_2 + H_2O \quad (3)$$

$$\equiv R - OH + OH^- = R \equiv O^- + H_2O \quad (4)$$

where ≡R represents the cell wall of the *Synechococcus* cell to which a proton-active surface functional group is attached. Eqs. (3) and (4) both correspond to site 3, as these two sites have been found to have similar pK_a values (Fein et al., 1997), however, it is best interpreted as an amino site, as hydroxyl sites with pK_a values ~10 generally occur only for phenol groups (Cox et al., 1999).

Previous studies have shown that the surface charge of the cell wall is strongly pH dependent; increasing pH drives the deprotonation of the organic ligands on the cell wall, leaving the cell wall with a net negative charge (e.g., Fein et al., 1997; Cox et al., 1999; Konhauser, 2007). Indeed, zeta potential measurements by Liu et al. (2015) determined that *Synechococcus* has a point of zero charge (PZC) below pH 4, and hence a net negative surface charge at marine pH. The negatively charged surface is composed of discrete surface sites that can bind metal cations, or act as nucleation sites for the growth of authigenic mineral phases (e.g. Konhauser et al., 1998).

The trend towards a net negative surface charge with increasing pH is mainly caused by the deprotonation of carboxyl and phosphoryl surface sites (reactions 1 and 2) below circumneutral pH. The positively charged amino groups are generally less abundant and have a smaller impact on the overall surface charge of the cell than either carboxyl or phosphoryl groups. This has been corroborated by titration results that indicate higher site densities for both the carboxyl (Site 1) and

Table 1
Potentiometric titration data in terms of site pKa, site concentration (mmol/g), and proposed functional group based on Liu et al., 2015.

Site	pKa	Site concentration (mol/g)	Functional group
1	5.59	2.389×10^{-3}	Carboxyl
2	7.61	1.244×10^{-3}	Phosphoryl
3	9.24	1.860×10^{-3}	Amino/Hydroxyl

phosphoryl (Site 2) ligands relative to the amino/hydroxyl groups (Site 3) Table 1.

3.2. Single metal adsorption experiments

3.2.1. Surface complexation modelling

The negatively charged, deprotonated sites on the cyanobacterial cells, resulting from an increased pH, act as loci for the binding of metal cations. Site pK_a values and ligand densities determined from the titration data were combined with pH edge metal adsorption data and hydrolysis constants from Baes and Mesmer (1976) (SI Tables 2a,b) to calculate the equilibrium metal binding constants using FITEQL. In this regard, a model that invoked metal binding to the carboxyl and phosphoryl groups best explains the experimental metal adsorption edge data. Metal binding to amino/hydroxyl groups were not important, as the pK_a value (9.24) was outside of the experimental range of the pH edge experiments, and even at pH 9, approximately 70% of these functional groups remain protonated. Mass action equations corresponding to each ligand can be used to predict the equilibrium state in more complex systems, including those in which multiple metals, compete for adsorption to bacterial surface functional groups (Fowle and Fein, 1999). The balanced chemical reactions for divalent cation (M^{2+}) adsorption onto carboxyl and phosphoryl groups, respectively, are:

$$\equiv R - COO^- + M^{2+} = \equiv R - COO - M^+ \quad (5)$$

$$\equiv R - PO_4H^- + M^{2+} = \equiv R - PO_4H - M^+ \quad (6)$$

with $\equiv$R representing the cellular surface to which functional group A is attached, and M representing the divalent metal cation. The metal binding constants (K) can be determined for each of the 2 sites in Eqs. (5) and (6) above as follows:

$$K = \frac{[\equiv R - COO - M^+]}{[[\equiv R - COO^-]a]_{M^{2+}}} \quad (7)$$

$$K = \frac{[\equiv R - PO_4H - M^+]}{[[\equiv R - PO_4H^-]a]_{M^{2+}}} \quad (8)$$

3.2.2. Metal adsorption to Synechococcus

Adsorption edges for trace metals to *Synechococcus* were generated for a pH range between 3 and 9 at an ionic strength of 0.56 M. Fig. 2(a–d) shows the percentage of each trace metal removed from solution by *Synechococcus*, plotted with the corresponding best-fit surface complexation model calculated in FITEQL. In all cases, at low pH, the organic cell wall functional groups are nearly completely protonated, and hence minimal adsorption of metal cations occurs. However, as pH increases, and functional groups progressively deprotonate, the now negatively-charged sites become available for cation binding. All metals investigated in this study reached maximum adsorption as pH approached 8.

Geochemical modelling using the programs PHREEQC and Geochemist's Workbench indicated that limited Cu and Co phases were above saturation, and no Ni or Zn phases occurred above saturation throughout the experimental conditions. These phases (malachite, azurite, tenorite, Co_3O_4), however, are characteristic of phases produced during the weathering of ore deposits or synthetic phases formed at high-temperature. Accordingly, we consider that these phases would not precipitate at our experimental conditions due to their low kinetic rates of formation, and therefore these phases would exert minimal influence on the adsorption of these trace metals by *Synechococcus*.

Synechococcus has differing affinities for each metal cation, as indicated by their thermodynamic binding constants presented in Table 2. Zn and Cu were most removed from the simulated seawater, followed by Ni and Co. This is consistent with the Irving-Williams series that describes the stability of complexes formed by divalent first-row transition metal cations, and how the stability generally increases across the period to a maximum stability at copper: Mn(II) < Fe(II) < Co (II) < Ni(II) < Cu(II) > Zn(II) (Irving and Williams, 1953). With regards to *Synechococcus*, we similarly observe that Zn and Cu form stronger biological complexes than do Ni and Co. Interestingly, Co and Ni form stronger bonds with the carboxyl groups than Zn and Cu, however, Zn and Cu complexes form stronger bonds with phosphoryl groups. Overall, the results suggest that removal of Zn and Cu would be favoured under marine conditions, a finding corroborated by studies of the Northeast Pacific Ocean, where over 99% of Cu and > 95% of Zn are organically complexed (Bruland, 1980; Coale and Bruland, 1988; Bruland et al., 2013).

Differing adsorption edge results were obtained for each individual metal cation, indicative of the relative affinity of each cation for cell surface functional groups. Comparing metal removal from solution at pH 8, which is representative of marine conditions, Zn adsorption reached nearly 100% (Fig. 2a), Cu reached approximately 75% (Fig. 2b), Ni approximately 40% (Fig. 2c), and Co ca. 35% (Fig. 2d). Importantly, the FITEQL models track well with the experimental data through pH 5–8, which is the key range for metal binding as the pK_a values for the carboxyl and phosphoryl groups lie within that range. Although these experiments were performed at a high ionic strength, similar to that of seawater, the work by Liu et al. (2015) indicated that ionic strength has a limited effect on Cd binding by *Synechococcus*. Furthermore, previous work has demonstrated that metal adsorption onto bacterial cell walls is a fully reversible process, and that the irreversible transport of the metals into the cell wall or cytoplasm does not occur to a meaningful extent over the time period of the adsorption reactions (Mullen et al., 1989; Fowle and Fein, 2000; Liu et al., 2015). Therefore, the values determined by the SCM are indicative of only metal adsorption to the surface, not assimilation by *Synechococcus* cells.

3.3. Competitive metal adsorption

The protonation constants, corresponding site concentrations, metal binding constants determined from models of single-metal adsorption experiments (Section 3.2), and the aqueous speciation of each metal (SI Table 2 a&b) were combined into one SCM. It was then used to predict the extent of adsorption in systems containing *Synechococcus* cells and all of the four metals. FITEQL models, along with the binding constants for the hydrolysis reactions, were utilized to solve for metal adsorption as a function of pH. The SCM predictions were then compared with the adsorption data from the experiments conducted at the same conditions to test the predictive rigour of the SCM. The competitive, multi-metal adsorption experiments were conducted using 2.5 ppm of each of the four metals in order to maintain a similar overall metal concentration (10 ppm) as the single element adsorption experiments.

The trends in cation affinity for *Synechococcus* observed in the competitive metal adsorption experiments are similar to those of the single metal experiments, with Zn showing the highest adsorption at pH 8 followed by Cu, Co, and Ni (Fig. 3). However, Cu removal appears to plateau at pH 7 in the single element pH edge, while in the multi-element system, adsorption plateaus at approximately pH 5.5, and subsequently drops below the Zn curve at pH 8. Based on the modelling output from FITEQL, this pattern reflects decreased Cu adsorption on each of the two functional sites, carboxyl and phosphoryl groups, which could be due to competition with other cations as pH increases. The

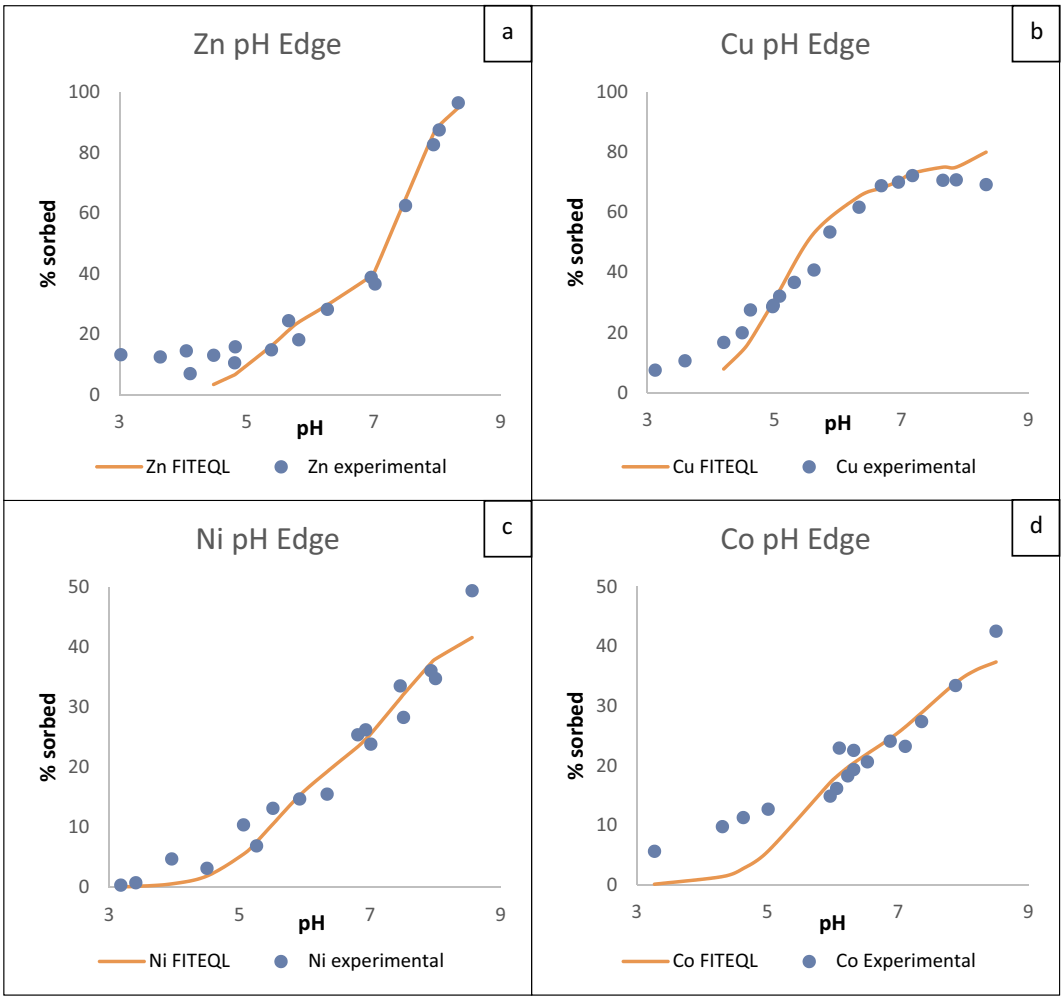

Fig. 2. (a–d): Zn pH edge in terms of % adsorption over the pH range studied, plotted alongside the FITEQL model.

Table 2
Binding constants for each metal-ligand complex determined by FITEQL modelling of titration and pH edge data.

Metal	Site 1 logK	Site 2 logK
Zn	4.365	7.863
Cu	3.726	7.412
Ni	4.667	6.097
Co	4.612	6.262

SCM accurately predicts Co, Ni, and Zn adsorption in the multi-metal system, while for Cu it predicts slightly weaker adsorption than is observed experimentally. The competitive sorption analysis provided here indicates that the relative sequestration of metals from the water column by *Synechococcus* was not significantly influenced by the presence of other trace metal ions, and that models based on single ion adsorption accurately predict the binding behaviour of *Synechococcus*.

4. Marine trace elements and their implications for the Precambrian

4.1. The importance of marine bioessential elements

Many of the trace elements in modern seawater are affected by the production and excretion of dissolved organic ligands, some of which are cyanobacterial in origin (e.g., Coale and Bruland, 1988; Dupont et al., 2004; Bruland et al., 2013). Once excreted, these ligands can complex metal cations, keeping them in solution and thus bioavailable. For example, extracellular, ferric iron-chelating ligands, such as siderophores, can scavenge and solubilize iron from seawater, making it available for microbial cells (Neilands, 1995; Boiteau et al., 2016). Similar ligands also exist for metals, such as Co, Cu, Mo, and Zn (Bruland et al., 2013). In contrast, other organic ligands are produced to reduce trace metal concentrations to below toxic levels (Bruland et al., 1991). For example, in the northeastern Pacific ocean, Cu binding ligands have been found to complex up to 99.7% of free Cu, significantly reducing its bioavailability and limiting its toxicity (Coale and Bruland, 1988).

Each of the metals chosen for this study represent important co-factors in metalloenzymes required for various important cellular processes such as photosynthesis, respiration, and DNA and RNA synthesis (e.g. Robbins et al. 2016). Zinc is a component in an array of metallopeptides and polymerases, and many Zn metalloenzymes are involved in DNA and RNA synthesis (Lipscomb and Sträter, 1996). Nuclear bound Zn is also important for eukaryotes in the so-called Zn-fingers, small protein structural motifs which act as signalling agents within the nucleus (e.g., Dupont et al., 2006; Dupont et al., 2010). Copper is found in more than thirty enzymes including those involved in metabolic reactions and methanogenesis (Chi Fru, 2011), as electron carriers in the thylakoid membrane during photosynthesis in cyanobacteria (Cavet et al., 2003), as well as in plastocyanin, ferrous oxidase, and amine oxidase (Morel et al., 2013). Nickel is critical for most bacteria, and can be found in hydrogenase, urease, and superoxide dismutase (Hausinger, 1987; Dupont et al., 2008). The foremost role of Co in biological utilization is as a cofactor in vitamin B12 (cobalamin), where a central

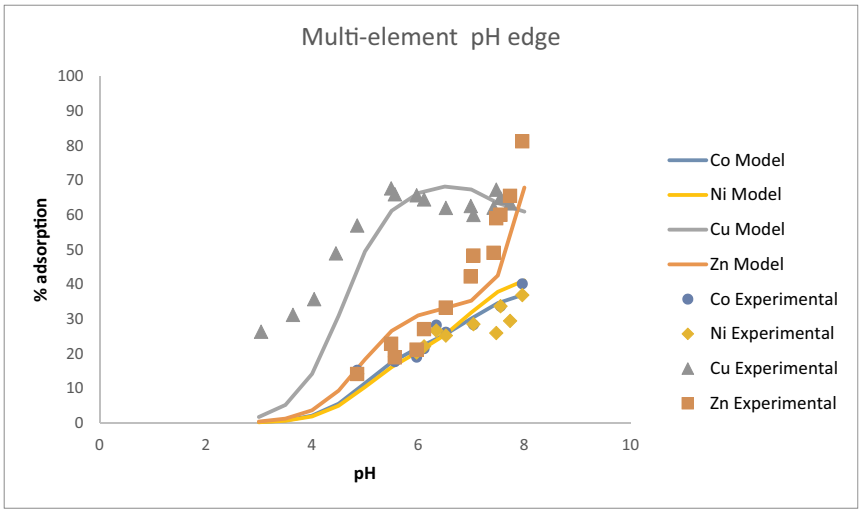

Fig. 3. Competitive adsorption of the 4 studied metals in terms of % adsorption, plotted alongside the predicted FITEQL model from the determined K values for each metal from the single element adsorption experiments.

cobalt atom is coordinated by four nitrogen ligands (Banerjee and Ragsdale, 2003). Eukaryotes use cobalamin in methionine synthesis (Swanner et al., 2014), while bacteria and archaea use cobalamin in enzymes for anaerobic metabolisms such as fermentation, dehalogenation, one-carbon compound electron transfers (Banerjee and Ragsdale, 2003), and in carbonic anhydrase (Morel et al., 2013).

In modern seawater, each of these metals show "nutrient-like" profiles, with decreased concentrations in the photic zone due to biological uptake, and increasing concentrations with depth as the metals are solubilized and returned to seawater as a consequence of cell biomass degradation (Bruland et al., 2013). However, Saito and Moffett (2002) have postulated that Co can behave as nutrient-like element at the surface due to biological uptake, however, with increasing depth, Co behaves as a scavenged type element as it does not show deep-water enrichment due to the oxidation of Co(II) to Co(III).

The concentrations and bioavailability of Zn, Cu, and Co in marine surface waters are all significantly influenced by speciation and complexation with dissolved organic ligands, as over 90% of each of these metals are organically complexed, causing the available concentrations to be significantly lower than the true concentrations (Hunter et al., 1997; Saito and Moffett, 2001; Ellwood and Van den Berg, 2001; Morel and Price, 2003; Leão et al., 2007; Bruland et al., 2013). This in marked contrast to Ni where only 10–30% of dissolved Ni is bound by organic complexes (Van Den Berg and Nimmo, 1987; Donat et al., 1994; Achterburg and Van Den Berg, 1997), while approximately 10% of Ni exists as chloride complexes, and 50% exists as the inorganic Ni^{2+} cation (Byrne, 2002).

Using realistic marine concentrations of trace metals and cyanobacterial cell densities, the amount of each cation that was adsorbed to *Synechococcus* can be estimated for the marine photic zone and compared to our experimental results to assess the effects of trace metal adsorption to *Synechococcus* on marine trace metal cycling. Seawater trace metal concentrations were acquired from Bruland et al. (2013) as follows: 300 pmol/kg Co, 12 nmol/kg Ni, 4.5 nmol/kg Cu, and 9 nmol/kg of Zn; while the seawater *Synechococcus* cell density was assumed to be 10^5 cells/mL. In the experiments, it was determined that 5 g L^{-1} wet mass contained approximately 1.2×10^{10} cells/mL based on cell counting using a haemocytometer. Based on the adsorption experiments at pH 8, a 10 mL *Synechococcus* culture of this density has the ability to adsorb approximately 5.9×10^{-5} mol of Co, 6.2×10^{-5} mol of Ni, 1.3×10^{-4} mol of Cu, and 1.3×10^{-4} mol of Zn. By dividing the amount of each metal adsorbed during the adsorption experiments by 1.2×10^{10} cells, it was determined that each *Synechococcus* cell had the ability to adsorb 4.92×10^{-15} mol of Co, 5.17×10^{-15} mol Ni, and 1.08×10^{-14} mol of both Cu and Zn. Based on these values and multiplying them by 10^5 cells mL^{-1} to simulate a marine *Synechococcus* bloom, the hypothetical amounts of the bioessential trace elements adsorbed in the water column could be calculated, which corresponds to removals of 4.92×10^{-8} mol of Co, 5.17×10^{-8} mol Ni, and 1.08×10^{-7} mol of Cu and Zn per L of seawater. Each of these values is higher than the corresponding trace metal seawater concentration, indicating that a *Synechoccocus*bloom could theoretically adsorb the entire seawater inventory of these trace metals.

Although these results demonstrate *Synechococcus* has the potential to be a significant trace metal sink, the effects of trace metal adsorption to marine DOC cannot be ignored. The marine DOC reservoir has been estimated to contain 200 times more carbon than oceanic biomass (Hansell et al. 2009), with the majority of trace metals being associated with these organic ligands. Recent research by Whitby et al. (2018) calculated the copper-ligand logK values for two ligand classes in the Northeast Pacific, with the value for the first ligand, L_1, being 15.0–16.5, and the second, L_2, measuring 11.6–13.6. These values are significantly higher than the values calculated in this study, and in order to illustrate how this affects trace metal adsorption, a predictive SCM with the incorporation of DOC was developed, as described in Section 3.2.2. In this predictive model, 5 ppm of Cu was used while an equivalent number of sites were incorporated for both the *Synechococcus* and DOC. The binding constants were derived from Whitby et al. (2018) for the DOC, and from the SCM for the *Synechococcus*. The input and output data for this predictive model are presented in SI Table 3(a–b).

Based on the predictive model, DOC adsorbs > 99.9% of the Cu while *Synechococcus* adsorbs < 0.1% of the Cu^{2+} at pH 8. This model is in agreement with the studies that indicate the majority of trace metals are associated with dissolved ligands in the modern oceans (e.g. Bruland et al. 2014). However, this study does demonstrate that bacterial surfaces have the capabilities to theoretically bind natural seawater concentrations of bioessential metals and that these sites could be important for trace metal cycling and their surface reactivity should be considered in future studies. Furthermore, the ability for *Synechococcus* to adsorb trace metals could have a much greater effect on trace metal cycling in ancient oceans, as discussed later in Section 4.2.

It is important to point out that the values for trace metal adsorption by the surface ligands of *Synechococcus* presented here are elevated compared to those for those recently in determined for *Rhodovulum iodosum* in Konhauser et al. (2018). This discrepancy could be due to one of several factors including; (i) the *R. iodosum* values modeled by Konhauser et al. (2018) were for cellular-mineral aggregates, i.e., cell

biomass and ferrihydrite mineral grains; (ii) binding constants in Konhauser et al. (2018) were extrapolated using a linear free energy approach, but for *Synechococcus* they were calculated from experimental metal adsorption data for use in surface complexation modelling; (iii) adsorption experiments performed here were at much higher levels of metal loading – 10 ppm as opposed to seawater concentrations; and (iv) Konhauser et al. (2018) assumed only carboxyl groups were binding the transition metals under paleomarine pH conditions, while here we also consider phosphoryl groups. When viewed in terms of metal absorbed per unit of biomass, differences between values generated herein and Konhauser et al. (2018) are within approximately two orders of magnitude, which may be accounted for in differences between extrapolated and modeled binding constants. Importantly, the values calculated in this study demonstrate that *Synechococcus* can adsorb significantly higher proportion of trace elements than present in seawater. These results also show that *Synechococcus* absorbs slightly higher, although similar amounts of these trace metals relative to Cd, which may adsorb approximately 10^{-16} mol per cell (Liu et al., 2015). This suggests that *Synechococcus* can potentially be a significant sink for these bioessential trace metals in the photic zone.

4.2. Implications for trace metal cycling and ancient ocean chemistry

The ability of cyanobacteria to effectively adsorb metal cations from seawater owes to their large surface area to volume ratio and rapid growth rates (Fisher, 1985). Phytoplankton biomass turns over on the order of once per week (Falkowski et al., 1998) to daily (Zhou et al., 2015a, b); consequently, trace metal cycling in the ocean is necessarily a rapid process in order to meet the trace metal demands of the oceanic biosphere. Although metals bound to the cell wall may eventually return to seawater at depths in the open ocean due to the bacterial degradation of organic matter (Sunda, 2012), it is possible that a fraction will settle to the relatively shallow continental shelves, carrying with them the adsorbed metals. This notion was postulated by Konhauser et al. (2002) for ancient iron rich sediments, where it was believed that trace metals would be immobilized with dead biomass and vectored to the accumulating sediment forming the precursor to banded iron formations (BIF). Each layer of dead biomass would be isolated by sedimenting Fe-rich particles, and therefore, trace-metal mobility would have been limited. As time progressed, the buried biomass would be respired, and the adsorbed metals would subsequently be released and adsorbed onto Fe-particles and thereby become incorporated into the rock record. Konhauser et al. (2018) subsequently suggested that most of the trace element assemblage preserved in BIF was biologically assimilated in the water column and, hence, phytoplankton may have controlled the trace-metal inventories of ancient seawater and sediment. However, that study did not constrain the quantitative effects that cyanobacteria (intact cells or their DOC) exerted on trace element cycling in the marine water column.

Understanding the possible exit fluxes for trace metals is a crucial component for predicting how trace metals were sequestered into ancient marine settings, and how this ultimately affected their expression in the rock record. With regards to BIF, numerous studies have utilized those iron-rich chemical sediments as proxies for the evolution of trace metal abundances in the ancient ocean (e.g., Bjerrum and Canfield, 2002; Chi Fru et al., 2016; Konhauser et al., 2007, 2009, 2011, 2015; Partin et al., 2013a; Robbins et al., 2013; Swanner et al., 2014; Warchola et al., 2018). Similarly, shales have also proven to be a useful record for trace elements from the Archean through to the modern (e.g., Chi Fru et al., 2016; Scott et al., 2008; Scott et al., 2013; Partin et al., 2013b; Playter et al., 2017). When these studies are combined with proteomic studies (e.g Dupont et al., 2006; Dupont et al., 2010; David and Alm, 2011) they help to determine environmental factors that may influence the timing and emergence of organisms such as cyanobacteria. To accurately assess the potential for cyanobacterial surfaces to act as an exit channel for trace metals in seawater to modern and ancient sediments, it is necessary to quantify the adsorptive capacity in dynamic, multicomponent systems. Thus, the surface complexation models developed here contribute to the understanding of adsorption of Zn, Cu, Co, and Ni to *Synechococcus*, and because *Synechococcus* can act as a sink for trace metals, trace element deposition in the BIF and shale record.

Furthermore, despite the wealth of knowledge gleaned from these trace metal records, the primary exit channel for trace elements to the sediments remains a debated, and critically studied topic. One of four possible scenarios can be envisioned for the removal of trace metals from the water column: (1) adsorption to sinking biomass, such as *Synechococcus* cells, (2) adsorption to ferric iron minerals such as ferrihydrite, $Fe(OH)_3$, which formed the precursor phase of BIF (Konhauser et al., 2018), (3) adsorption to clay particles which form shales and fine grained siliciclastics in modern and ancient marine settings (e.g.: Playter et al., 2017), or (4) complexation with dissolved organic carbon which can either decrease trace metals' bioavailability or form aggregates which then settle to the seafloor (Engel et al., 2004). These four mechanisms need not be mutually exclusive, and a combination of one or more may contribute to the formation of ancient or modern sediments. This study demonstrates that cyanobacteria can adsorb appreciable amounts of bioessential trace metals from seawater. It also demonstrates that surface complexation modelling can be used to accurately predict the adsorption behaviour of cations in competitive systems, which is important for building predictive models to study the fluxes of cations in the marine water column. These two findings, taken together, serve to increase our understanding of trace metal fluxes in seawater by constraining the major trace nutrients cycling pathways.

Although this study shows that surface-bound organic ligands on *Synechococcus* can adsorb trace elements from seawater, their binding constants are lower than those of dissolved organic compounds in the ocean (e.g. Whitby et al., 2018). Based on the predictive model illustrating the differences in the adsorption of Cu to *Synechococcus* and DOC, dissolved organic ligands in the ocean do have a more significant effect on trace metal cycling and should be considered, along with particulates such as bacteria, clay particles, and iron oxides, as vectors controlling trace metal bioavailability in the oceans.

5. Conclusion

This study determined the ability of the marine cyanobacterium *Synechococcus* sp. PCC 7002 to remove biologically important metal cations (Co, Cu, Ni, Zn) from solution by adsorption using a surface complexation modelling approach. It was demonstrated that this species of cyanobacteria can adsorb considerable quantities of bioessential trace elements from simulated seawater, and importantly, we quantified the effects of competitive adsorption. The data shows that *Synechococcus* has the highest removal capacity for Cu and Zn, followed by Co and Ni. The ability for *Synechococcus* to remove trace metals were broadly consistent with the well-known Irving-Williams stability series for organic-metal complexes.

Our data indicate that *Synechococcus* has the potential to be a crucial contributor of the cycling of trace metals in the oceans due to adsorption to the cell surface. Additional mechanisms which may contribute to metal removal include complexation with Cl^- or OH^- species, precipitation as hydroxides or carbonates at high pH, or competition for adsorption by other dissolved ligands, bacteria, or particulate matter in the water column. Nevertheless, this study corroborates the hypothesis that phytoplankton are ideally suited to scavenge trace metals from seawater due to their rapid growth and correspondent cellular turnover rates, high surface area to volume ratio, and highly reactive cell walls.

This study is one of the first to quantitatively investigate competitive adsorption of bioessential trace metals to marine biomass, and future work should focus on assessing additional exit channels for the incorporation of these nutrients into BIF pre-cursor phases such as ferrihydrite and silica, dissolved organic carbon, and bacterial

assimilation. By determining the metal binding behaviour of trace elements to particulate matter in seawater, including multi-metal, multi-sorbent systems, models containing multiple sorbents and metals, which more closely represent realistic marine conditions, can be developed. By assessing a range of realistic sorbent and metal concentrations, this competitive SCM approach will allow for further refinement of the role of specific exit pathways on the cycling of trace elements between the water column and sediments in both modern and ancient marine systems, and ultimately for the identification of transition metal-based biosignatures within the rock record.

Acknowledgements

This work was supported by a Natural Sciences and Engineering Research Council of Canada (NSERC) Discovery Grant 165831 to K.O.K, 04134 to D.S.A., and 171319 to G.W.O. TJW gratefully acknowledges a NSERC Canada Graduate Scholarship (CGS) – Masters, and LJR a NSERC Vanier CGS.

The authors declare no competing interests.

Appendix A. Supplementary data

Supplementary data to this article can be found online at https://doi.org/10.1016/j.chemgeo.2019.05.021.

References

Achterburg, E.P., Van Den Berg, C.M.G., 1997. Chemical speciation of chromium and nickel in the western Mediterranean. Deep Sea Res. Part 2 44, 693–720.
Alam, Md S., Swaren, L., von Gunten, K., Cossio, M., Bishop, B., Robbins, L.J., Hou, D., Flynn, S.L., Ok, Y.S., Konhauser, K.O., Alessi, D.S., 2018. Application of surface complexation modeling to trace metals uptake by biochar-amended agricultural soils. Appl. Geochem. 88, 103–112.
Alessi, D.S., Henderson, J.M., Fein, J.B., 2010. Experimental measurement of monovalent cation adsorption onto Bacillus subtilis cells. Geomicrobiol J. 27, 464–472.
Anderson, T.R., Tang, K.W., 2010. Carbon cycling and POC turnover in the mesopelagic zone of the ocean: Insights from a simple model. Deep. Res. Part II Top. Stud. Oceanogr. 57, 1581–1592.
Azam, F., Fenchel, T., Field, J.G., Gray, J.S., Meyer-Reil, L.A., Thingstad, F., 1983. The ecological role of water-column microbes in the sea. Mar. Ecol. Prog. Ser. 10, 257–263.
Baes, C.F., Mesmer, R.E., 1976. The Hydrolysis of Cations. vol. 489 John Wiley and Sons Inc., Oakridge National Laboratory.
Banerjee, R., Ragsdale, S.W., 2003. The many faces of vitamin B12: catalysis by cobalamin-dependent enzymes1. Annu. Rev. Biochem. 72, 209–247.
Bethke, C.M., Brady, P.V., 2000. How the Kd approach undermines ground water cleanup. Groundwater 38, 435–443.
Bjerrum, C.J., Canfield, D.E., 2002. Ocean productivity before about 1.9 Gyr ago limited by phosphorus adsorption onto iron oxides. Nature 417, 159–162.
Boiteau, R.M., Mende, D.R., Hawco, N.J., McIlvin, M.R., Fitzsimmons, J.N., Saito, M.A., Sedwick, P.N., DeLong, E.F., Repeta, D.J., 2016. Siderophore-based microbial adaptations to iron scarcity across the eastern Pacific Ocean. Proc. Natl. Acad. Sci. 113, 14237–14242.
Borrok, D., Turner, B.F., Fein, J.B., 2005. A universal surface complexation framework for modeling proton binding onto bacterial surfaces in geologic settings. Am. J. Sci. 305, 826–853.
Bruland, K.W., 1980. Oceanographic distributions of cadmium, zinc, nickel, and copper in the North Pacific. Earth Planet. Sci. Lett. 47, 176–198.
Bruland, K.W., Donat, J.R., Hutchins, D.A., 1991. Interactive influences of bioactive trace metals on biological production in oceanic waters. Limnol. Oceanogr. 36, 1555–1577.
Bruland, K.W., Middag, R., Lohan, M.C., 2013. Controls of Trace Metals in Seawater. In: Treatise on Geochemistry, Second edition. pp. 19–51.
Byrne, R.H., 2002. Inorganic speciation of dissolved elements in seawater: the influence of pH on concentration ratios. Geochem. Trans. 2, 11.
Carlson, C.A., Hansell, D.A., 2014. DOM sources, sinks, reactivity, and budgets. In: Biogeochemistry of Marine Dissolved Organic Matter, 2nd ed. Elsevier Inc.
Cavet, J.S., Borrelly, G.P.M., Robinson, N.J., 2003. Zn, Cu and Co in cyanobacteria: selective control of metal availability. FEMS Microbiol. Rev. 27, 165–181.
Chi Fru, E., 2011. Copper biogeochemistry: a cornerstone in aerobic methanotrophic bacterial ecology and activity? Geomicrobiol J. 28, 601–614.
Chi Fru, E., Rodríguez, N.P., Partin, C.A., Lalonde, S.V., Andersson, P., Weiss, D.J., El Albani, A., Rodushkin, I., Konhauser, K.O., 2016. Cu isotopes in marine black shales record the Great Oxidation Event. Proc. Natl. Acad. Sci. 113, 4941–4946.
Coale, K.H., Bruland, K.W., 1988. Copper complexation in the Northeast Pacific. Limnol. Oceanogr. 33, 1084–1101.
Cox, J.S., Smith, D.S., Warren, L.A., Ferris, F.G., 1999. Characterizing heterogeneous bacterial surface functional groups using discrete affinity spectra for proton binding. Environ. Sci. Technol. 33, 4514–4521.
David, L.A., Alm, E.J., 2011. Rapid evolutionary innovation during an Archaean genetic expansion. Nature 469, 93–96.
Dittrich, M., Sibler, S., 2005. Cell surface groups of two picocyanobacteria strains studied by zeta potential investigations, potentiometric titration, and infrared spectroscopy. J. Colloid and Interface Sci. 286, 487–495.
Donat, J.R., Lao, K.A., Bruland, K.W., 1994. Speciation of dissolved copper and nickel in South San Francisco Bay: a multi-method approach. Anal. Chim. Acta 284, 547–571.
Dupont, C.L., Nelson, R.K., Bashir, S., Moffett, J.W., Ahner, B.A., 2004. Novel copper-binding and nitrogen-rich thiols produced and exuded by Emiliania huxleyi. Limnol. Oceanogr. 49, 1754–1762.
Dupont, C.L., Yang, S., Palenik, B., Bourne, P.E., 2006. Modern proteomes contain putative imprints of ancient shifts in trace metal geochemistry. Proc. Natl. Acad. Sci. U. S. A. 103, 17822–17827.
Dupont, C.L., Neupane, K., Shearer, J., Palenik, B., 2008. Diversity, function and evolution of genes coding for putative Ni-containing superoxide dismutases. Environ. Microbiol. 10, 1831–1843.
Dupont, C.L., Butcher, A., Valas, R.E., Bourne, P.E., Caetano-Anollés, G., 2010. History of biological metal utilization inferred through phylogenomic analysis of protein structures. Proc. Natl. Acad. Sci. 107, 10567–10572.
Ellwood, M.J., Van den Berg, C.M.G., 2001. Determination of organic complexation of cobalt in seawater by cathodic stripping voltammetry. Mar. Chem. 75, 33–47.
Engel, A., Thoms, S., Riebesell, U., Rochelle-Newall, E., Zondervan, I., 2004. Polysaccharide aggregation as a potential sink of marine dissolved organic carbon. Nature 428, 929–932.
Falkowski, P.G., Barber, R.T., Smetacek, V., 1998. Biogeochemical controls and feedbacks on ocean primary production. Science 281, 200–206.
Fein, J.B., 2006. Thermodynamic Modeling of Metal Adsorption onto Bacterial Cell Walls: Current Challenges. Adv. Agron. 90, 179–202.
Fein, J.B., 2017. Advanced biotic ligand models: using surface complexation modeling to quantify metal bioavailability to bacteria in geologic systems. Chem. Geol. 464, 127–136.
Fein, J.B., Daughney, C.J., Yee, N., Davis, T.A., 1997. A chemical equilibrium model for metal adsorption onto bacterial surfaces. Geochim. Cosmochim. Acta 61 (16), 3319–3328.
Fisher, N.S., 1985. Accumulation of metals by marine phytoplankton. Mar. Biol. 87, 137–142.
Flombaum, P., Gallegos, J.L., Gordillo, R.A., Rincon, J., Zabala, L.J., Jiao, N., Karl, D.M., Li, W.K., Lomas, M.W., Veneziano, D., 2013. Present and future distributions of the marine cyanobacteria *Prochlorococcus* and *Synechococcus*. Proc. Natl. Acad. Sci. U. S. A. 110, 9824–9829.
Flynn, S.L., Szymanowski, J.E.S., Fein, J.B., 2014. Modeling bacterial metal toxicity using a surface complexation approach. Chem. Geol. 374–375, 110–116.
Fowle, D.A., Fein, J.B., 1999. Competitive adsorption of metal cations onto two gram positive bacteria: Testing the chemical equilibrium model. Geochim. Cosmochim. Acta 63, 3059–3067.
Fowle, D.A., Fein, J.B., 2000. Experimental measurements of the reversibility of metal-bacteria adsorption reactions. Chem. Geol. 168, 27–36.
Gélabert, A., Pokrovsky, O.S., Schott, J., Feurtet-Mazel, A., 2018. Surface complexation modeling of interactions between freshwater and marine diatom species and trace elements (Mo, W, Cr, Ge, Ga, Al). Chem. Geol. 494, 117–126.
Hadjoudja, S., Deluchat, V., Baudu, M., 2010. Cell surface characterization of *Microcystis aeruginosa* and *Chlorella vulgaris*. J. Colloid Interface Sci. 342, 293–299.
Hansell, D., Carlson, C., Repeta, D., Schlitzer, R., 2009. Dissolved Organic Matter in the Ocean: A Controversy Stimulates New Insights. Oceanography 22, 202–211.
Hausinger, R.P., 1987. Nickel utilization by microorganisms. Microbiol. Rev. 51, 22–42.
Herbelin, A.L., Westall, J.C., 1999. FITEQL 4.0: A Computer Program for Determination of Chemical Equilibrium Constants from Experimental Data.
Huisman, J., Codd, G.A., Paerl, H.W., Ibelings, B.W., Verspagen, J.M.H., Visser, P.M., 2018. Cyanobacterial blooms. Nat. Rev. Microbiol. 16, 471–483.
Hunter, K.A., Kim, J.P., Croot, P.L., 1997. Biological roles of trace metals in natural waters. Environ. Monit. Assess. 44, 103–147.
Irving H. and Williams R. J. P. (1953). The stability of transition-metal complexes. J. Chem. Soc. 0, 3192–3210.
Jiang, W., Saxena, A., Song, B., Ward, B.B., Beveridge, T.J., Myneni, S.C.B., 2004. Elucidation of functional groups on gram-positive and gram-negative bacterial surfaces using infrared spectroscopy. Langmuir 20, 11433–11442.
Konhauser, K.O., 2007. Introduction to Geomicrobiology. Blackwell, Oxford.
Konhauser, K.O., Fisher, Q.J., Fyfe, W.S., Longstaffe, F.J., Powell, M.A., 1998. Authigenic mineralization and detrital clay binding by freshwater biofilms: the Brahmani river, India. Geomicrobiol J. 15, 209–222.
Konhauser, K.O., Hamade, T., Raiswell, R., Morris, R.C., Ferris, F.G., Southam, G., Canfield, D.E., 2002. Could bacteria have formed the Precambrian banded iron formations? Geology 30, 1079–1082.
Konhauser, K.O., Lalonde, S.V., Amskold, L., Holland, H.D., 2007. Was there really an Archean phosphate crisis? Science Brevia 315, 1234.
Konhauser, K.O., Pecoits, E., Lalonde, S.V., Papineau, D., Nisbet, E.G., Barley, M.E., Arndt, N.T., Zahnle, K., Kamber, B.S., 2009. Oceanic nickel depletion and a methanogen famine before the Great Oxidation Event. Nature 458, 750–753.
Konhauser, K.O., Lalonde, S.V., Planavsky, N.J., Pecoits, E., Lyons, T.W., Mojzsis, S.J., Rouxel, O.J., Barley, M.E., Rosiere, C., Fralick, P.W., Kump, L.R., Bekker, A., 2011. Aerobic bacterial pyrite oxidation and acid rock drainage during the Great Oxidation Event. Nature 478, 369–373.
Konhauser, K.O., Robbins, L.J., Pecoits, E., Peacock, C., Kappler, A., Lalonde, S.V., 2015. The Archean nickel famine revisited. Astrobiology 15, 804–815.
Konhauser, K.O., Robbins, L.J., Alessi, D.S., Flynn, S.L., Gingras, M.K., Martinez, R.E.,

Kappler, A., Swanner, E.D., Li, Y.L., Crowe, S.A., Planavsky, N.J., Reinhard, C.T., Lalonde, S.V., 2018. Phytoplankton contributions to the trace-element composition of Precambrian banded iron formations. Bull. Geol. Soc. Am. 130, 941–951.
Konhauser, K.O., Hao, W., Li, Y., Gunten, K., Bishop, B.A., Alessi, D.S., Tarhan, L.G., 2019. Diopatra cuprea worm burrow parchment: a cautionary tale of infaunal surface reactivity. Lethaia. https://doi.org/10.1111/let.12335.
Koretsky, C., 2000. The significance of surface complexation reactions in hydrologic systems: a geochemist's perspective. J. Hydrol. 230, 127–171.
Lalonde, S.V., Smith, D.S., Owttrim, G.W., Konhauser, K.O., 2008a. Acid-base properties of cyanobacterial surfaces I: influences of growth phase and nitrogen metabolism on cell surface reactivity. Geochim. Cosmochim. Acta 72, 1257–1268.
Lalonde, S.V., Smith, D.S., Owttrim, G.W., Konhauser, K.O., 2008b. Acid-base properties of cyanobacterial surfaces. II: silica as a chemical stressor influencing cell surface reactivity. Geochim. Cosmochim. Acta 72, 1269–1280.
Lalonde, S.V., Dafoe, L.T., Pemberton, S.G., Gingras, M.K., Konhauser, K.O., 2010. Investigating the geochemical impact of burrowing animals: Proton and cadmium adsorption onto the mucus lining of Terebellid polychaete worms. Chem. Geol. 271, 44–51.
Leão, P.N., Vasconcelos, M.T.S.D., Vasconcelos, V.M., 2007. Role of marine cyanobacteria in trace metal bioavailability in seawater. Microb. Ecol. 53, 104–109.
Lipscomb, W.N., Sträter, N., 1996. Recent advances in zinc enzymology. Chem. Rev. 96, 2375–2433.
Liu, Y., Alessi, D.S., Owttrim, G.W., Petrash, D.A., Mloszewska, A.M., Lalonde, S.V., Martinez, R.E., Zhou, Q., Konhauser, K.O., 2015. Cell surface reactivity of Synechococcus sp. PCC 7002: implications for metal sorption from seawater. Geochim. Cosmochim. Acta 169, 30–44.
Martinez, R.E., Konhauser, K.O., Paunova, N., Wu, W., Alessi, D.S., Kappler, A., 2016. Surface reactivity of the anaerobic phototrophic Fe(II)-oxidizing bacterium Rhodovulum iodosum: implications for trace metal budgets in ancient oceans and banded iron formations. Chem. Geol. 442, 113–120.
Moffett, J.W., Brand, L.E., 1996. Production of strong, extracellular Cu chelators by marine cyanobacteria in response to Cu stress. Limnol. Oceanogr. 41 (3), 388–395.
Morel, F.M.M., 2008. The co-evolution of phytoplankton and trace element cycles in the oceans. Geobiology 6, 318–324.
Morel, F.M.M., Price, N., 2003. The biogeochemical cycles of trace metals in the ocean. Science 300, 944–947.
Morel, F.M.M., Hudson, R.J.M., Price, N.M., 1991. Limitation of productivity by trace metals in the sea. Limnol. Oceanogr. 36 (8), 1742–1755.
Morel, F.M.M., Milligan, A.J., Saito, M.A., 2013. Marine bioinorganic chemistry: the role of trace metals in the oceanic cycles of major nutrients. In: Treatise on Geochemistry: Second Ed. vol. 8. pp. 123–150.
Mullen, M.D., Wolf, D.C., Ferris, F.G., Beveridge, T.J., Flemming, C.A., Bailey, G.W., 1989. Bacterial sorption of heavy metals. Appl. Environ. Microbiol. 55, 3143–3149.
Neilands, J.B., 1995. Siderophores: structure and function of microbial iron transport compounds. J. Biol. Chem. 270, 26723–26726.
Partin, C.A., Lalonde, S.V., Planavsky, N.J., Bekker, A., Rouxel, O.J., Lyons, T.W., Konhauser, K.O., 2013a. Uranium in iron formations and the rise of atmospheric oxygen. Chem. Geol. 362, 82–90.
Partin, C.A., Bekker, A., Planavsky, N.J., Scott, C.T., Gill, B.C., Li, C., Podkovyrov, V., Maslov, A., Konhauser, K.O., Lalonde, S.V., Love, G.D., Poulton, S.W., Lyons, T.W., 2013b. Large-scale fluctuations in Precambrian atmospheric and oceanic oxygen levels from the record of U in shales. Earth Planet. Sci. Lett. 369-370, 284–293.
Petrash, D.A., Lalonde, S.V., Gingras, M.K., Konhauser, K.O., 2011. A surrogate approach to studying the chemical reactivity of burrow mucous linings in marine sediments. Palaios 26, 594–600.
Playter, T., Konhauser, K., Owttrim, G., Hodgson, C., Warchola, T., Mloszewska, A.M., Sutherland, B., Bekker, A., Zonneveld, J.P., Pemberton, S.G., Gingras, M., 2017. Microbe-clay interactions as a mechanism for the preservation of organic matter and trace metal biosignatures in black shales. Chem. Geol. 459, 75–90.
Price, N.M., Morel, F.M.M., 1990. Cadmium and cobalt substitution for zinc in a marine diatom. Nature 344, 658–660.
Robbins, L.J., Lalonde, S.V., Saito, M.A., Planavsky, N.J., Mloszewska, A.M., Pecoits, E., Scott, C., Dupont, C.L., Kappler, A., Konhauser, K.O., 2013. Authigenic iron oxide proxies for marine zinc over geological time and implications for eukaryotic metallome evolution. Geobiol 11, 295–306.
Robbins, L.J., Lalonde, S.V., Planavsky, N.J., Partin, C.A., Reinhard, C.T., Kendall, B., Scott, C., Hardisty, D.S., Gill, B.C., Alessi, D.S., Dupont, C.L., Saito, M.A., Crowe, S.A., Poulton, S.W., Bekker, A., Lyons, T.W., Konhauser, K.O., 2016. Trace elements at the intersection of marine biological and geochemical evolution. Earth-Science Rev 163, 323–348.
Saito, M.A., Moffett, J.W., 2001. Complexation of cobalt by natural organic ligands in the Sargasso sea as determined by a new high-sensitivity electrochemical cobalt speciation method suitable for open ocean work. Mar. Chem. 75, 49–68.
Saito, M.A., Moffett, J.W., 2002. Temporal and spatial variability of cobalt in the Atlantic Ocean. Geochim. Cosmochim. Acta 66, 1943–1953.
Sañudo-Wilhelmy, S.A., Tovar-Sanchez, A., Fu, F., Capone, D.G., Carpenter, E.J., Hutchins, D.A., 2004. The impact of surface-adsorbed phosphorus on phytoplankton Redfield stoichiometry. Nature 432, 897–901.
Scott, C., Lyons, T.W., Bekker, A., Shen, Y., Pouton, S.W., Chu, X., Anbar, A.D., 2008. Tracing the stepwise oxygenation of the Proterozoic ocean. Nature 452, 456–459.
Scott, C., Planavsky, N.J., Dupont, C.L., Kendall, B., Gill, B.C., Robbins, L.J., Husband, K.F., Arnold, G.L., Wing, B.A., Poulton, S.W., Bekker, A., Anbar, A.D., Konhauser, K.O., Lyons, T.W., 2013. Bioavailability of zinc in marine systems through time. Nat. Geosci. 6, 125–128.
Stevens, S.E., Porter, R.D., 1980. Transformation in *Agmenellum quadriplicatum*. Proc. Natl. Acad. Sci. U. S. A. 77, 6052–6056.
Stevens, S., Van Baalen, C., 1973. Characteristics of nitrate reductions in a mutant of the blue-green alga *Agmenellum quadruplicatum*. Plant Physiol. 51, 350–356.
Sunda, W.G., 2012. Feedback interactions between trace metal nutrients and phytoplankton in the ocean. Front. Microbiol. 3, 1–22.
Swanner, E.D., Planavsky, N.J., Lalonde, S.V., Robbins, L.J., Bekker, A., Rouxel, O.J., Saito, M.A., Kappler, A., Mojzsis, S.J., Konhauser, K.O., 2014. Cobalt and marine redox evolution. Earth Planet. Sci. Lett. 390, 253–263.
Twining, B.S., Baines, S.B., 2013. The trace metal composition of marine phytoplankton. Annu. Rev. Mar. Sci. 5, 191–215.
Van Den Berg, C.M.G., Nimmo, M., 1987. Determination of interactions of nickel with dissolved organic material in seawater using cathodic stripping voltammetry. Sci. Total Environ. 60, 185–195.
Warchola, T.J., Flynn, S.L., Robbins, L.J., Liu, Y., Gauger, T., Kovalchuk, O., Alam Md, S., Wei, S., Myers, R., Bishop, B., Lalonde, S.V., Gingras, M.K., Kappler, A., Alessi, D.S., Konhauser, K.O., 2017. Field- and lab-based potentiometric titrations of microbial mats from the Fairmont hot spring. Geomicrobiol J. 34, 851–863.
Warchola, T., Lalonde, S.V., Pecoits, E., von Gunten, K., Robbins, L.J., Alessi, D.S., Philippot, P., Konhauser, K.O., 2018. Petrology and geochemistry of the Boolgeeda Iron Formation, Hamersley Basin, Western Australia. Precambrian Res. 316, 155–173.
Waterbury, J.B., Watson, S.W., Guillard, R.R.L., Brand, L.E., 1979. Widespread occurrence of a unicellular, marine, planktonic, cyanobacterium. Nature 277, 293–294.
Whitby, H., Posacka, A.M., Maldonado, M.T., 2018. Copper-binding ligands in the NE Pacific. Mar. Chem. 204, 36–48.
Worden, A.Z., Nolan, J.K., Palenik, B., 2004. Assessing the dynamics and ecology of marine picophytoplankton: the importance of the eukaryotic component. Limnol. Oceanogr. 49, 168–179.
Worms, I., Simon, D.F., Hassler, C.S., Wilkinson, K.J., 2006. Bioavailability of trace metals to aquatic microorganisms: importance of chemical, biological and physical processes on biouptake. Biochimie 88, 1721–1731.
Yee, N., Benning, L.G., Phoenix, V.R., Ferris, F.G., 2004. Characterization of metal-cyanobacteria sorption reactions: a combined macroscopic and infrared spectroscopic investigation. Environ. Sci. Technol. 38, 775–782.
Zhou, L., Tan, Y., Huang, L., Hu, Z., Ke, Z., 2015a. Seasonal and size-dependent variations in the phytoplankton growth and microzooplankton grazing in the southern South China Sea under the influence of the East Asian monsoon. Biogeosciences 12, 6809–6822.
Zhou, L., Tan, Y., Huang, L., Li, G., 2015b. Does microzooplankton grazing contribute to the pico-phytoplankton dominance in subtropical and tropical oligotrophic waters. Acta Ecol. Sin. 35, 29–38.